Figure S1

A

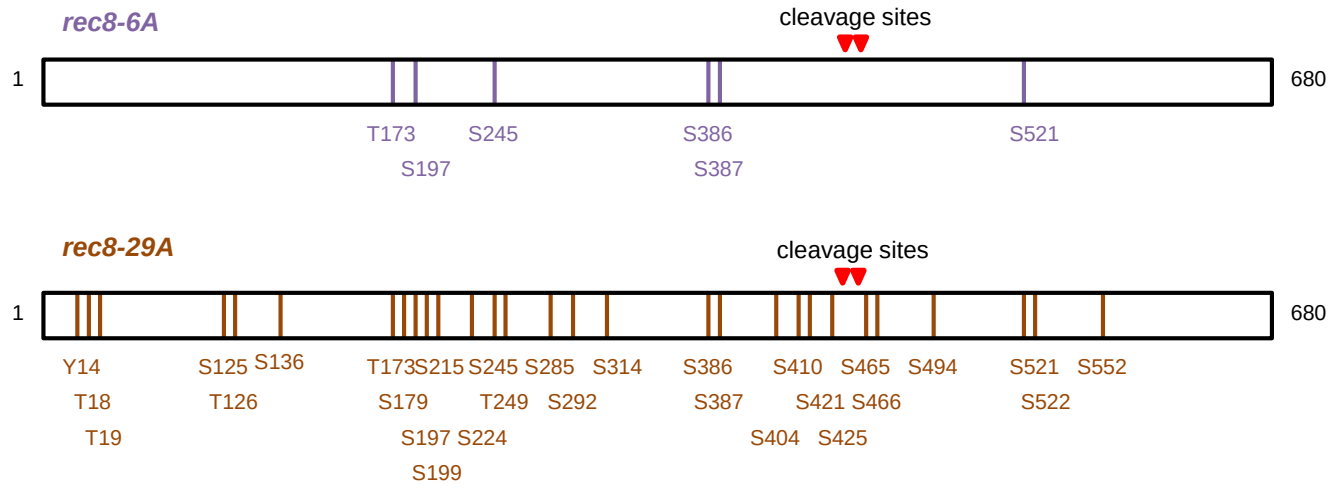
rec8-6A
cleavage sites
1
680
T173
S197
S245
S386
S387
S521
rec8-29A
cleavage sites
1
680
Y14
T18
T19
S125
S136
T126
T173
S179
S197
S199
S215
S224
S245
T249
S285
S292
S314
S386
S387
S404
S410
S421
S425
S465
S466
S494
S521
S522
S552

B

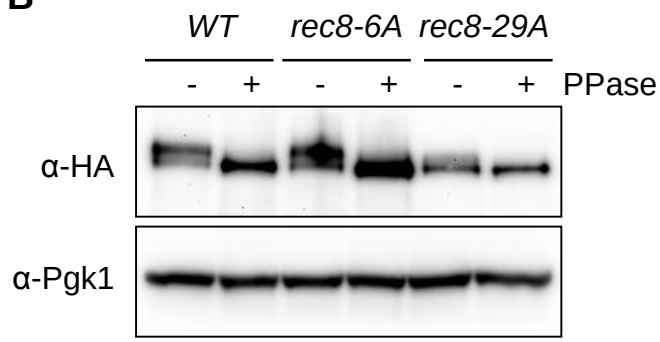
WT
rec8-6A
rec8-29A
- + - + - + PPase
α-HA
α-Pgk1

Figure S2

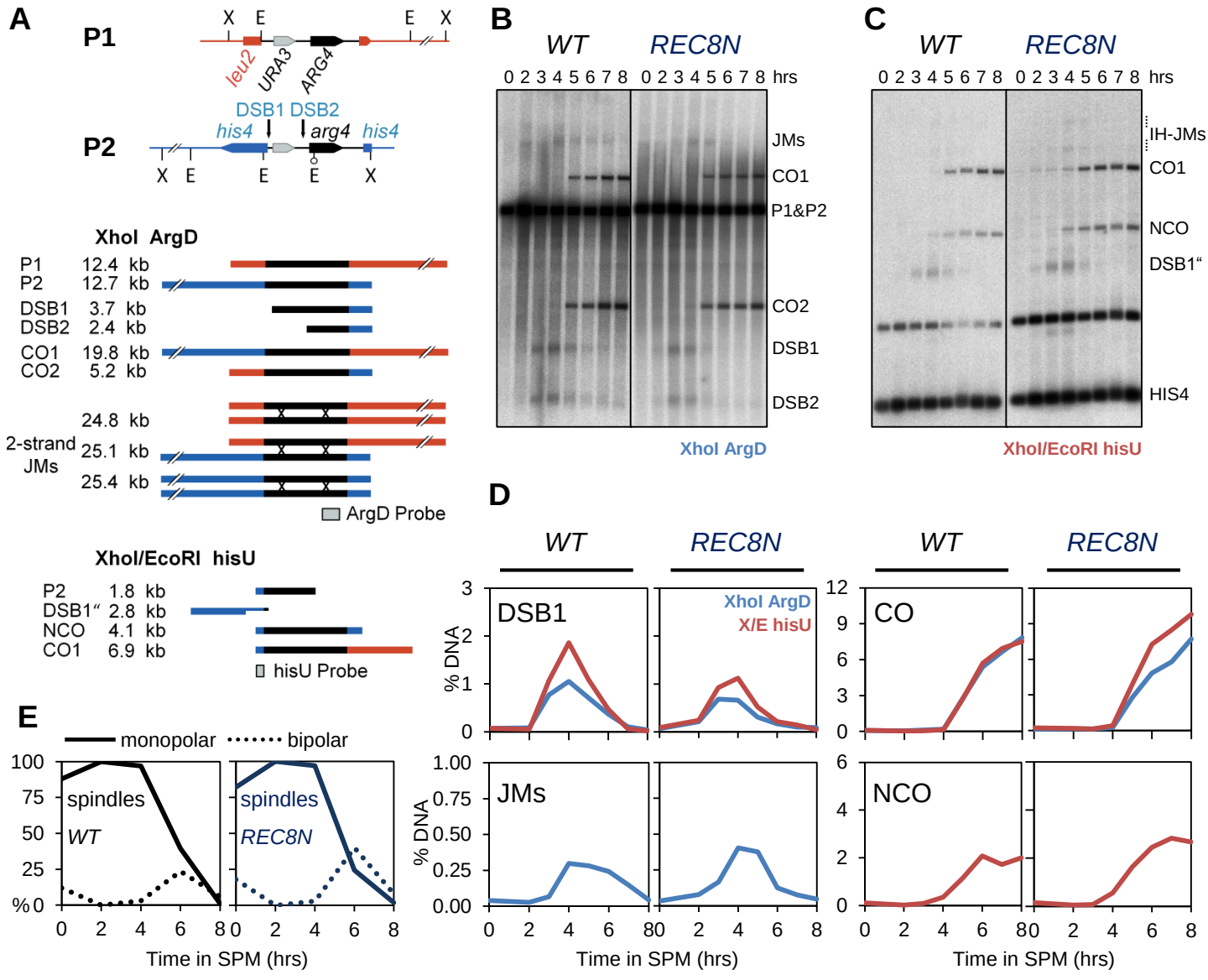
A
P1
X E E X
leu2 URA3 ARG4
DSB1 DSB2
P2
his4 arg4 his4
X E E E X
XhoI ArgD
P1 12.4 kb
P2 12.7 kb
DSB1 3.7 kb
DSB2 2.4 kb
CO1 19.8 kb
CO2 5.2 kb
24.8 kb
2-strand JMs
25.1 kb
25.4 kb
ArgD Probe
XhoI/EcoRI hisU
P2 1.8 kb
DSB1“ 2.8 kb
NCO 4.1 kb
CO1 6.9 kb
hisU Probe
B
WT REC8N
0 2 3 4 5 6 7 8 0 2 3 4 5 6 7 8 hrs
JMs
CO1
P1&P2
CO2
DSB1
DSB2
XhoI ArgD
C
WT REC8N
0 2 3 4 5 6 7 8 0 2 3 4 5 6 7 8 hrs
IH-JMs
CO1
NCO
DSB1“
HIS4
XhoI/EcoRI hisU
D
WT REC8N WT REC8N
DSB1
XhoI ArgD
X/E hisU
CO
JMs
NCO
% DNA
Time in SPM (hrs)
E
monopolar bipolar
spindles
WT
REC8N
% 0 25 50 75 100
0 2 4 6 8
Time in SPM (hrs)

Figure S3

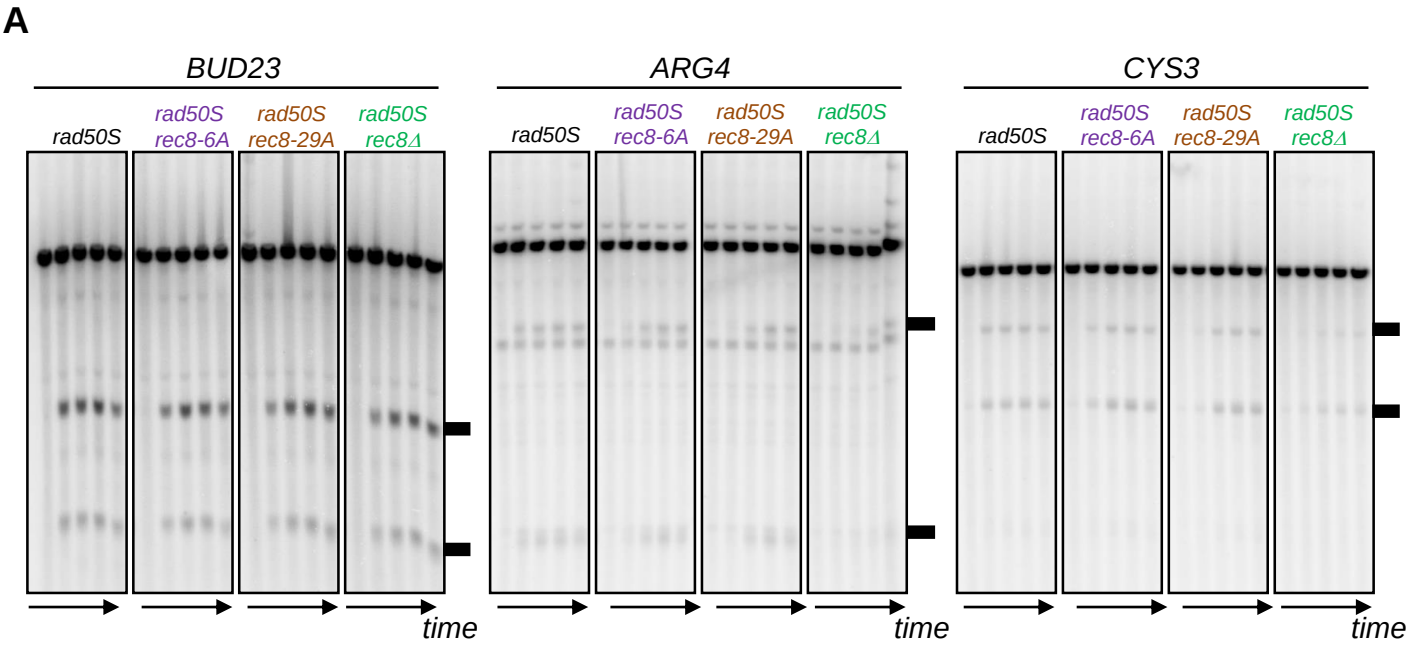
A
BUD23
ARG4
CYS3
rad50S
rad50S rec8-6A
rad50S rec8-29A
rad50S rec8Δ
time

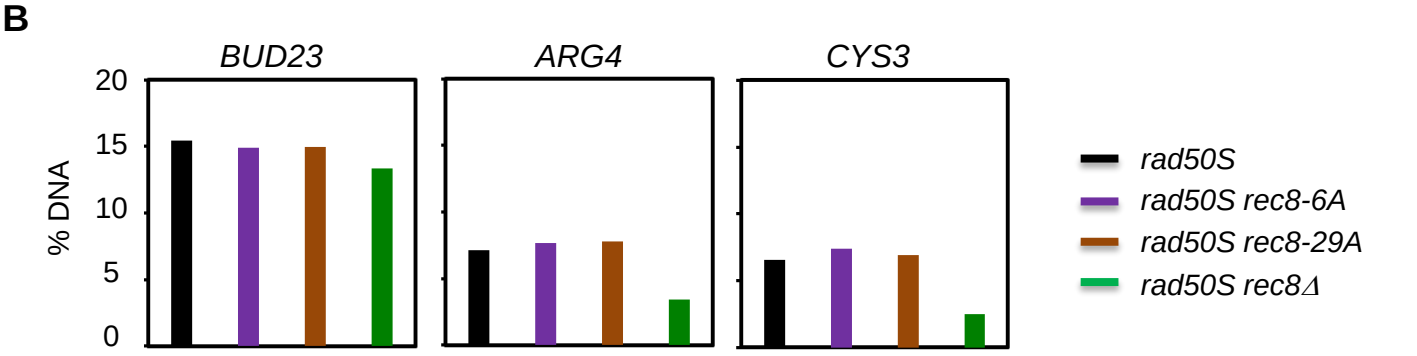
B
BUD23
ARG4
CYS3
% DNA
20
15
10
5
0
rad50S
rad50S rec8-6A
rad50S rec8-29A
rad50S rec8Δ

Figure S4

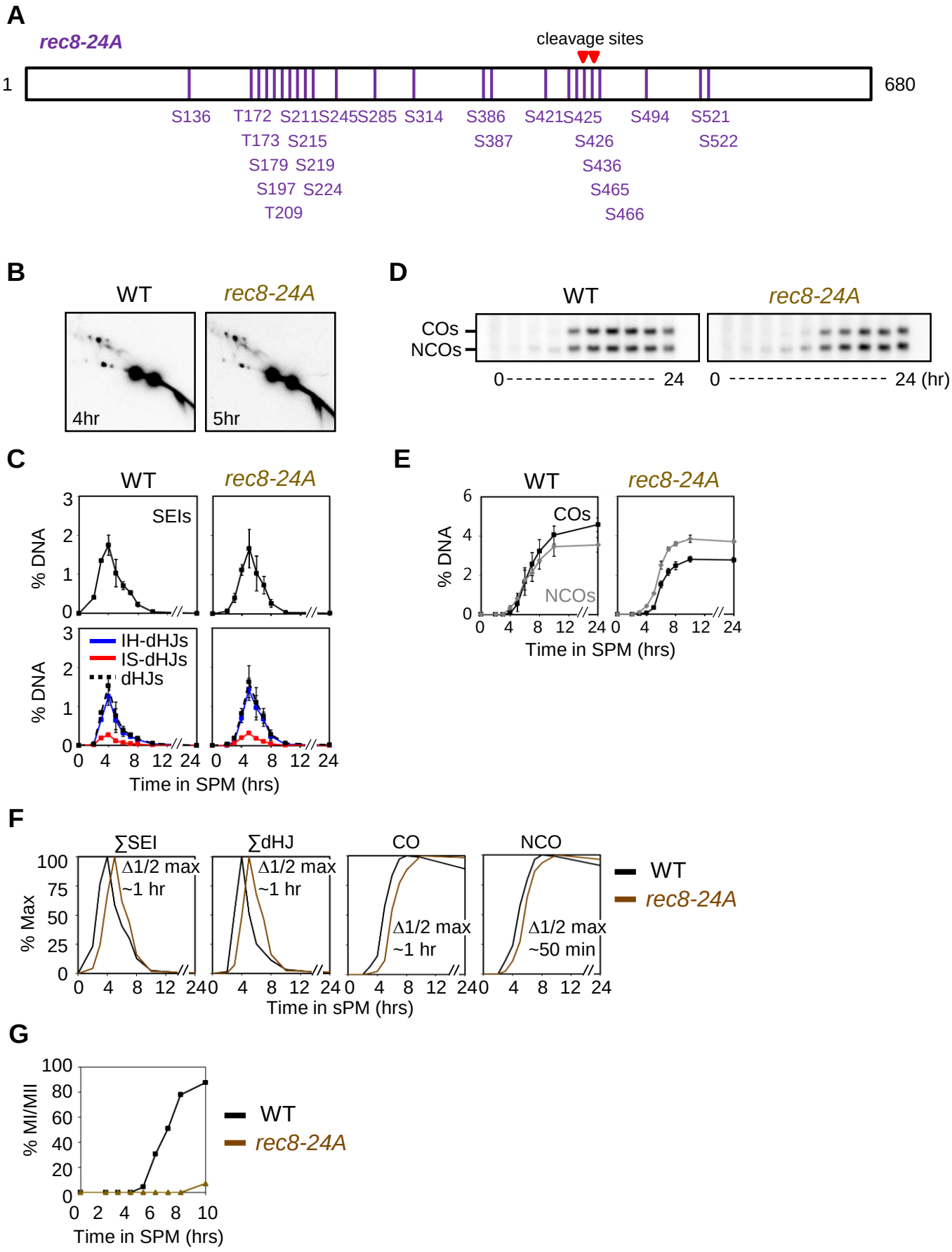
A
rec8-24A
cleavage sites
1
680
S136
T172 S211S245S285 S314
T173 S215
S179 S219
S197 S224
T209
S386
S387
S421S425
S426
S436
S465
S466
S494
S521
S522
B
WT
rec8-24A
4hr
5hr
D
WT
rec8-24A
COs
NCOs
0 24
0 24 (hr)
C
WT
rec8-24A
SEIs
% DNA
IH-dHJs
IS-dHJs
dHJs
Time in SPM (hrs)
E
WT
rec8-24A
COs
NCOs
% DNA
Time in SPM (hrs)
F
∑SEI
∑dHJ
CO
NCO
Δ1/2 max
~1 hr
Δ1/2 max
~50 min
% Max
WT
rec8-24A
Time in sPM (hrs)
G
% MI/MII
WT
rec8-24A
Time in SPM (hrs)

Figure S5

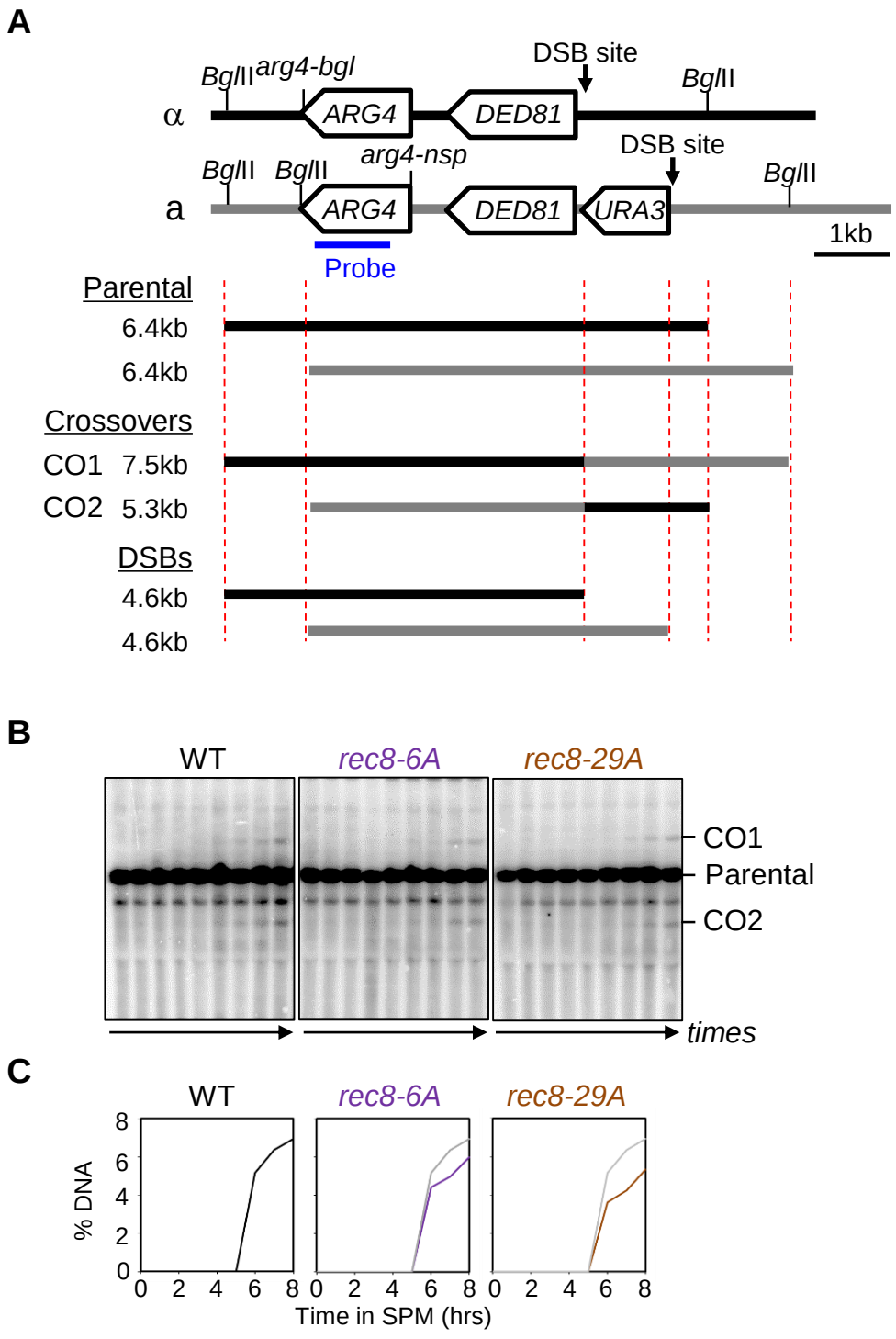
A
BglII
arg4-bgl
DSB site
BglII
α
ARG4
DED81
BglII
BglII
arg4-nsp
DSB site
BglII
a
ARG4
DED81
URA3
1kb
Probe
Parental
6.4kb
6.4kb
Crossovers
CO1 7.5kb
CO2 5.3kb
DSBs
4.6kb
4.6kb
B
WT
rec8-6A
rec8-29A
CO1
Parental
CO2
times
C
WT
rec8-6A
rec8-29A
% DNA
0
2
4
6
8
Time in SPM (hrs)

Figure S6

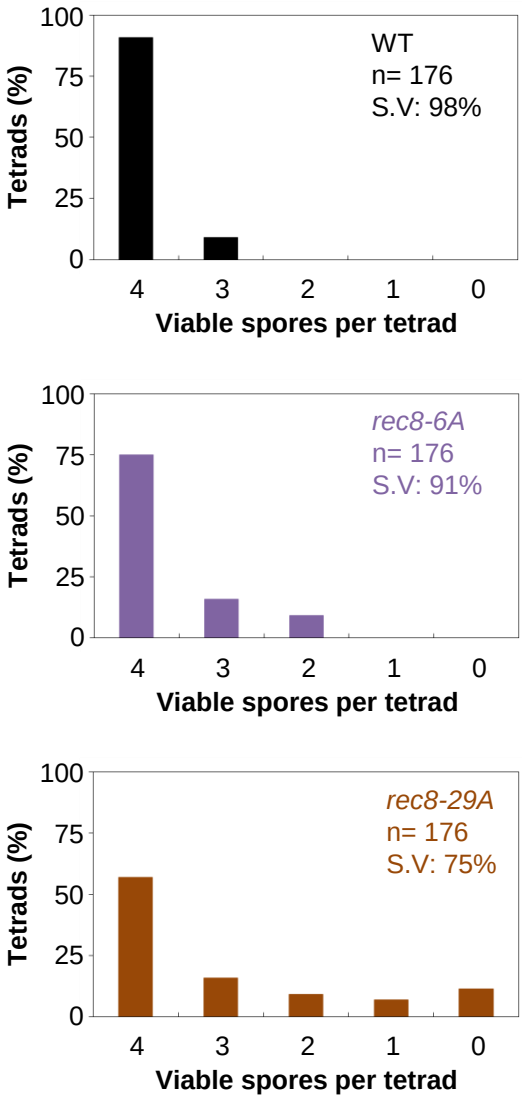
100
75
50
25
0
Tetrads (%)
WT
n= 176
S.V: 98%
4
3
2
1
0
Viable spores per tetrad
100
75
50
25
0
Tetrads (%)
rec8-6A
n= 176
S.V: 91%
4
3
2
1
0
Viable spores per tetrad
100
75
50
25
0
Tetrads (%)
rec8-29A
n= 176
S.V: 75%
4
3
2
1
0
Viable spores per tetrad

Figure S7

A

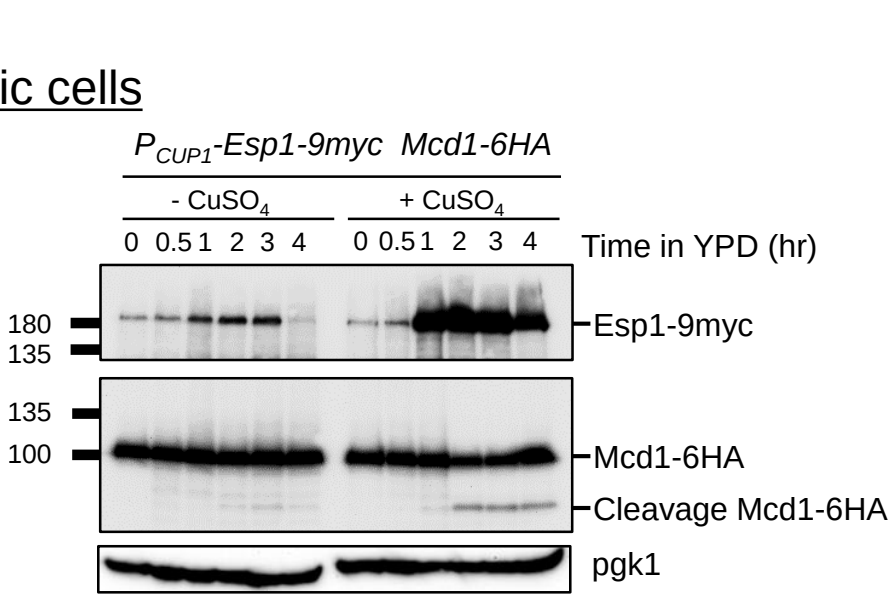
Mitotic cells
P_{CUP1}-Esp1-9myc Mcd1-6HA
- $CuSO_4$
+ $CuSO_4$
0 0.5 1 2 3 4 0 0.5 1 2 3 4
Time in YPD (hr)
180
135
Esp1-9myc
135
100
Mcd1-6HA
Cleavage Mcd1-6HA
pgk1

B

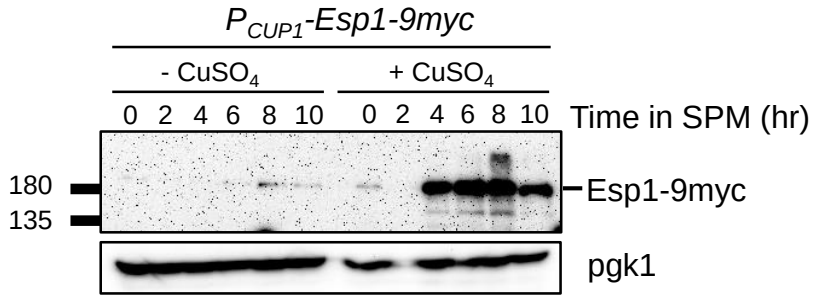
Meiotic cells
P_{CUP1}-Esp1-9myc
- $CuSO_4$
+ $CuSO_4$
0 2 4 6 8 10 0 2 4 6 8 10
Time in SPM (hr)
180
135
Esp1-9myc
pgk1

Figure S8

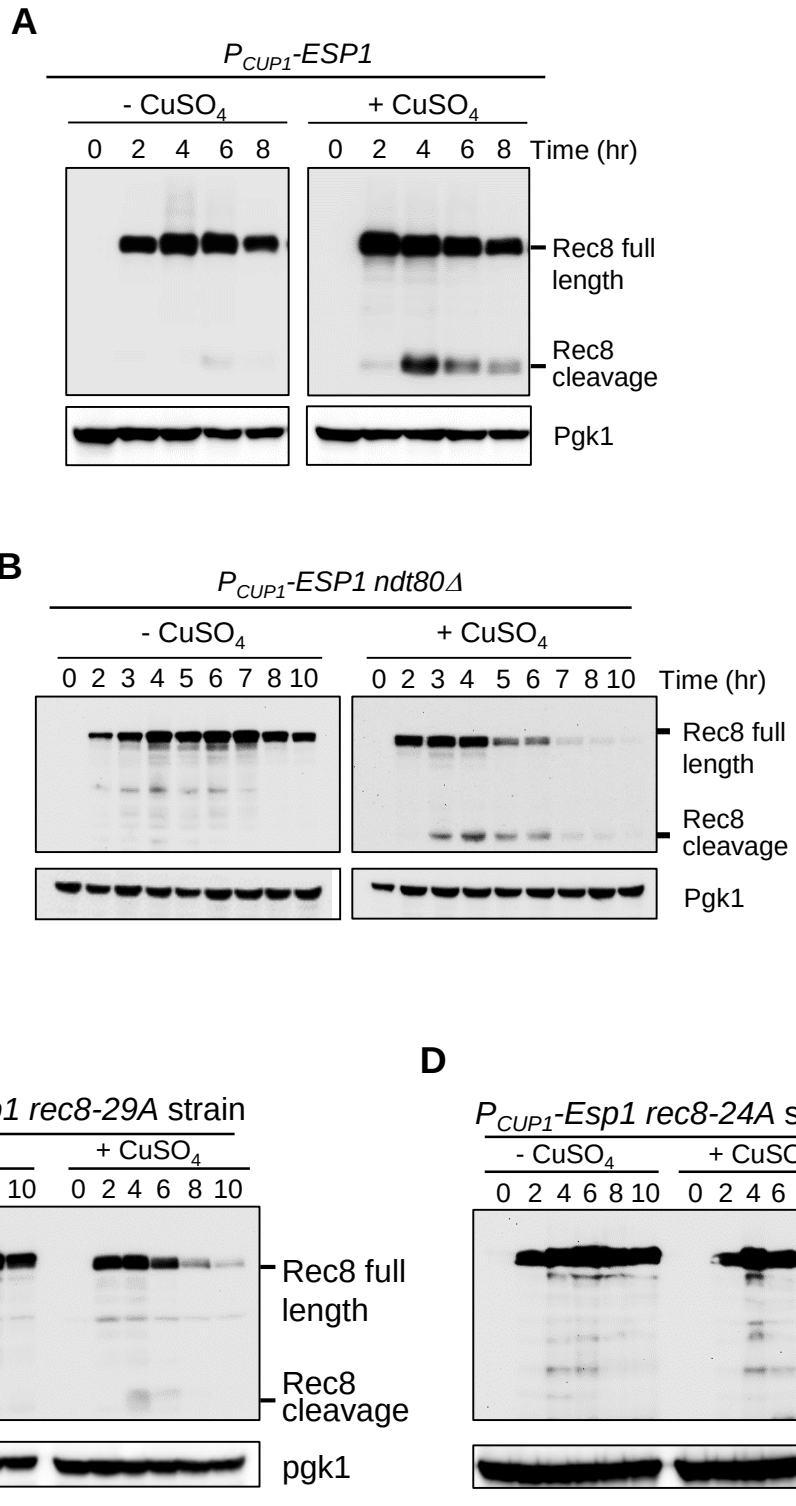
A
P_{CUP1}-ESP1
- $CuSO_4$
+ $CuSO_4$
0 2 4 6 8
0 2 4 6 8
Time (hr)
Rec8 full length
Rec8 cleavage
Pgk1
B
P_{CUP1}-ESP1 ndt80Δ
- $CuSO_4$
+ $CuSO_4$
0 2 3 4 5 6 7 8 10
0 2 3 4 5 6 7 8 10
Time (hr)
Rec8 full length
Rec8 cleavage
Pgk1
C
P_{CUP1}-Esp1 rec8-29A strain
- $CuSO_4$
+ $CuSO_4$
0 2 4 6 8 10
0 2 4 6 8 10
Rec8 full length
Rec8 cleavage
pgk1
D
P_{CUP1}-Esp1 rec8-24A strain
- $CuSO_4$
+ $CuSO_4$
0 2 4 6 8 10
0 2 4 6 8 10
Rec8 full length
Rec8 cleavage
pgk1

Figure S9

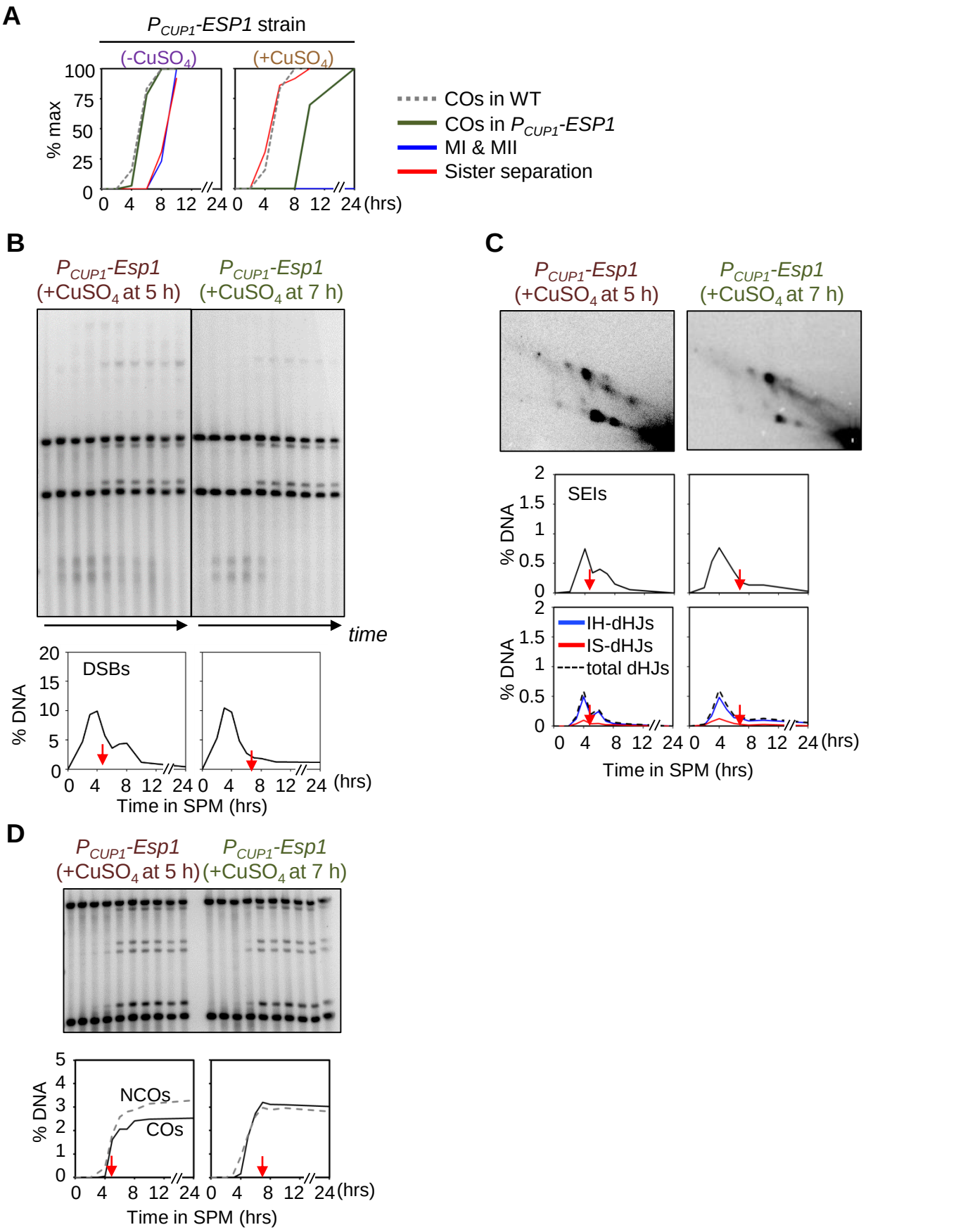
A
P_CUP1-ESP1 strain
(-CuSO4)
(+CuSO4)
% max
100
75
50
25
0
0 4 8 12 24 0 4 8 12 24 (hrs)
COs in WT
COs in P_CUP1-ESP1
MI & MII
Sister separation
B
P_CUP1-Esp1 (+CuSO4 at 5 h)
P_CUP1-Esp1 (+CuSO4 at 7 h)
time
DSBs
% DNA
20
15
10
5
0
0 4 8 12 24 0 4 8 12 24 (hrs)
Time in SPM (hrs)
C
P_CUP1-Esp1 (+CuSO4 at 5 h)
P_CUP1-Esp1 (+CuSO4 at 7 h)
SEIs
% DNA
2
1.5
1
0.5
0
IH-dHJs
IS-dHJs
total dHJs
0 4 8 12 24 0 4 8 12 24 (hrs)
Time in SPM (hrs)
D
P_CUP1-Esp1 (+CuSO4 at 5 h)
P_CUP1-Esp1 (+CuSO4 at 7 h)
% DNA
5
4
3
2
1
0
NCOs
COs
0 4 8 12 24 0 4 8 12 24 (hrs)
Time in SPM (hrs)

Figure S10

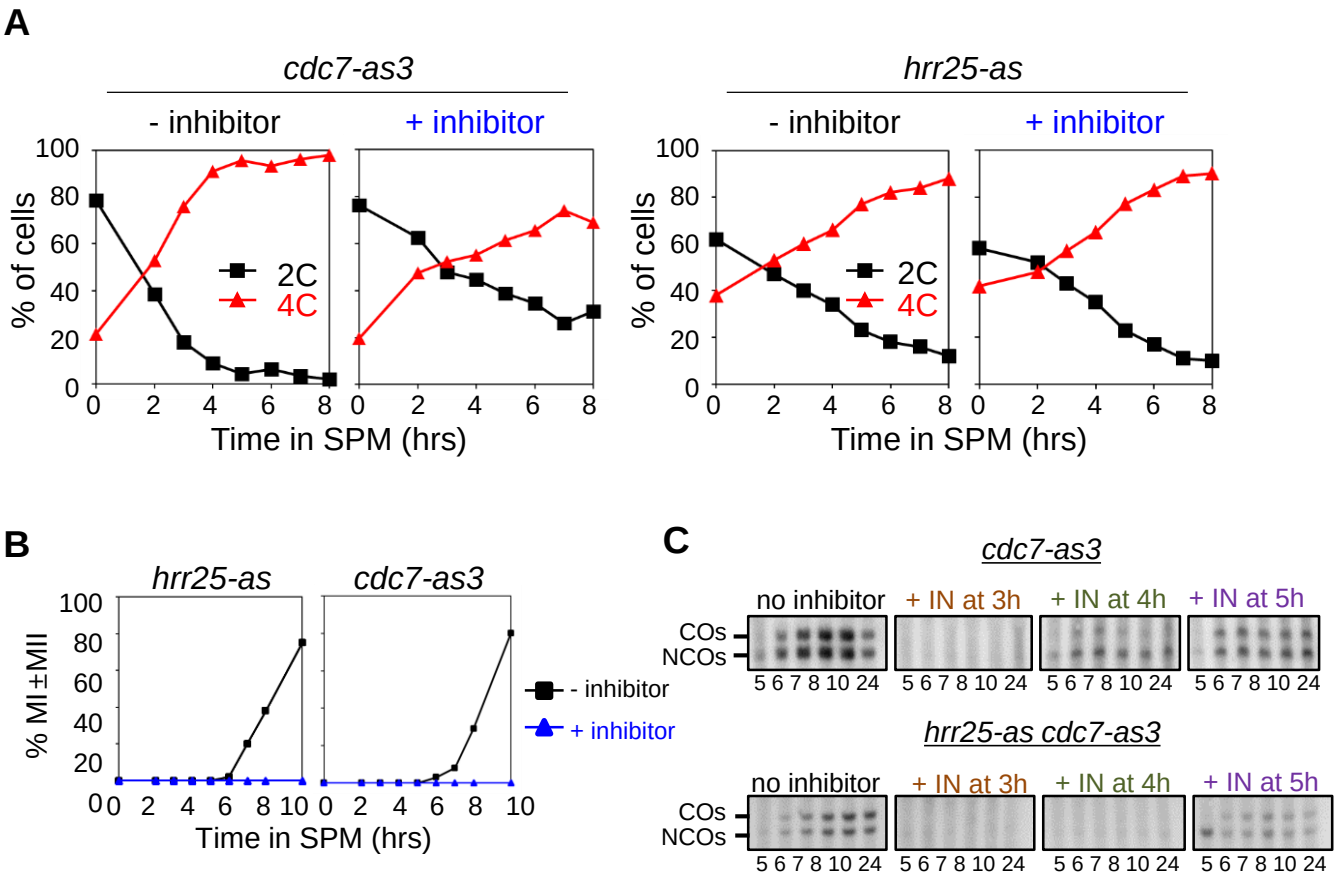
A
cdc7-as3
- inhibitor
+ inhibitor
hrr25-as
- inhibitor
+ inhibitor
% of cells
2C
4C
Time in SPM (hrs)
B
hrr25-as
cdc7-as3
% MI±MII
- inhibitor
+ inhibitor
Time in SPM (hrs)
C
cdc7-as3
no inhibitor
+ IN at 3h
+ IN at 4h
+ IN at 5h
COs
NCOs
5 6 7 8 10 24
hrr25-as cdc7-as3

Figure S11

ndt80Δ P_{CUP1}*-CDC5* strain

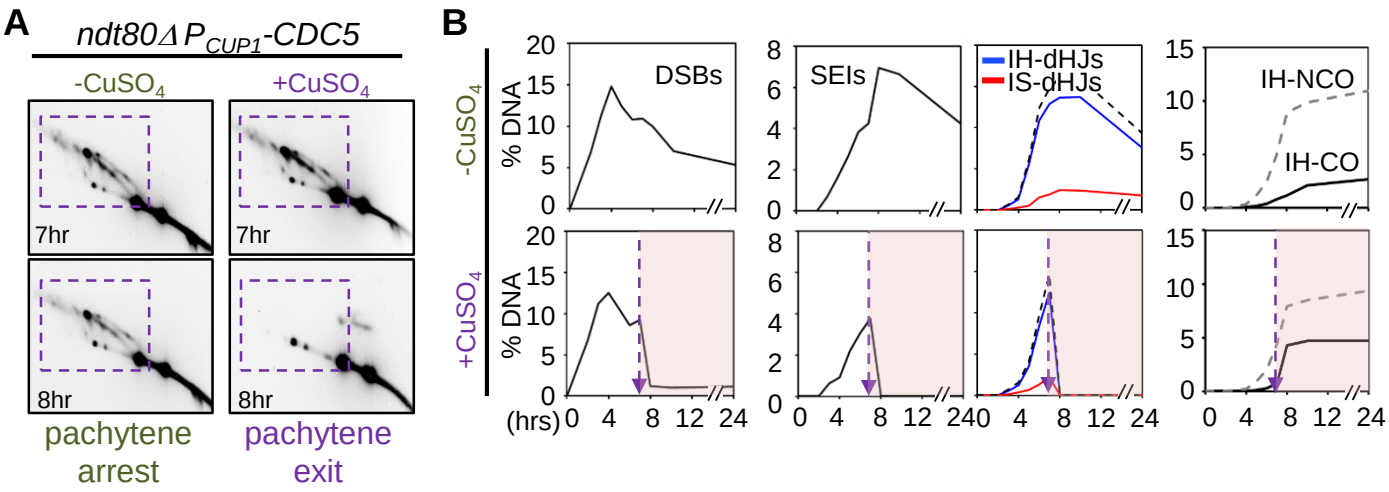

Figure S12

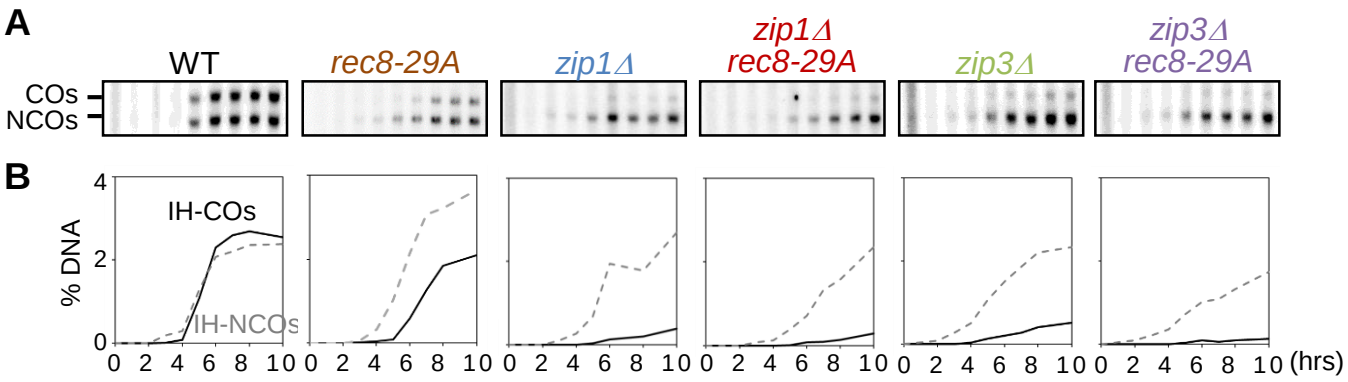
A
WT
rec8-29A
zip1Δ
zip1Δ rec8-29A
zip3Δ
zip3Δ rec8-29A
COs
NCOs
B
% DNA
IH-COs
IH-NCOs
0
2
4
0 2 4 6 8 10
(hrs)

Figure S13

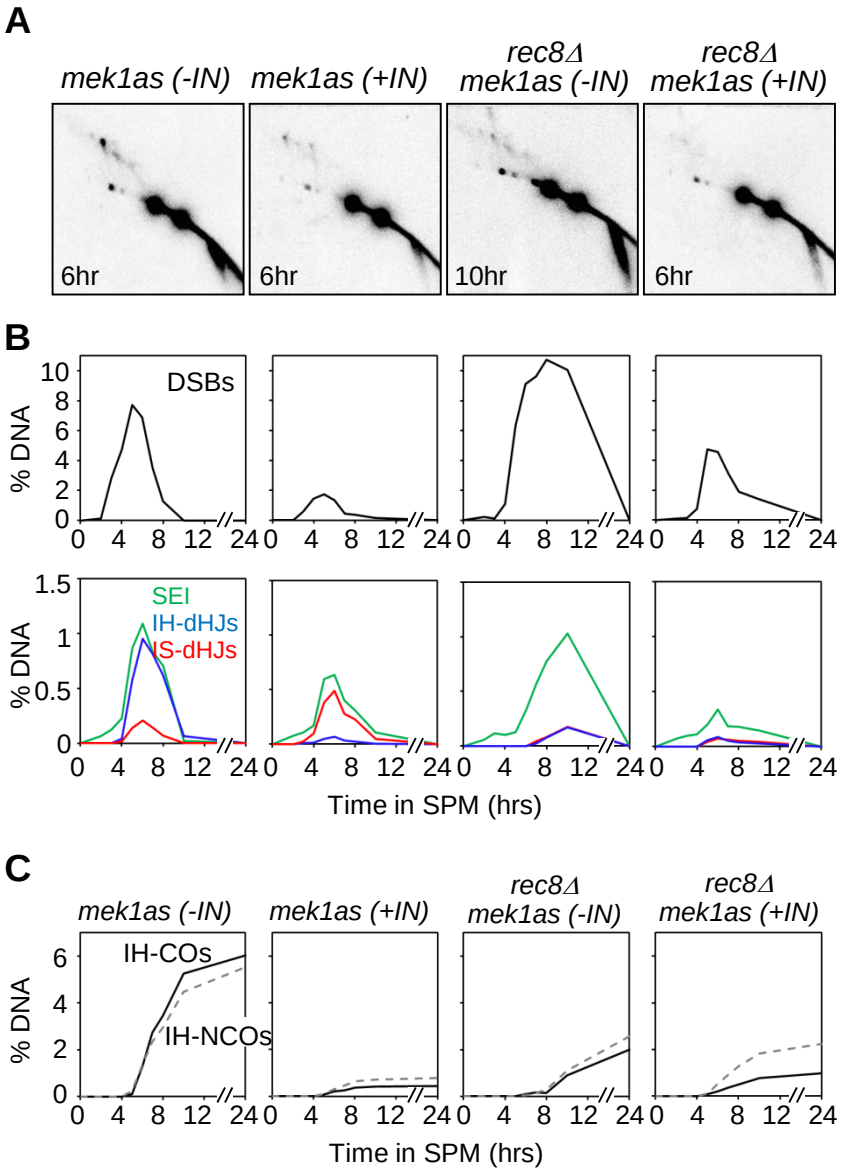
A
mek1as (-IN)
mek1as (+IN)
rec8Δ mek1as (-IN)
rec8Δ mek1as (+IN)
6hr
6hr
10hr
6hr
B
DSBs
% DNA
SEI
IH-dHJs
IS-dHJs
Time in SPM (hrs)
C
IH-COs
IH-NCOs
% DNA
Time in SPM (hrs)

Figure S14

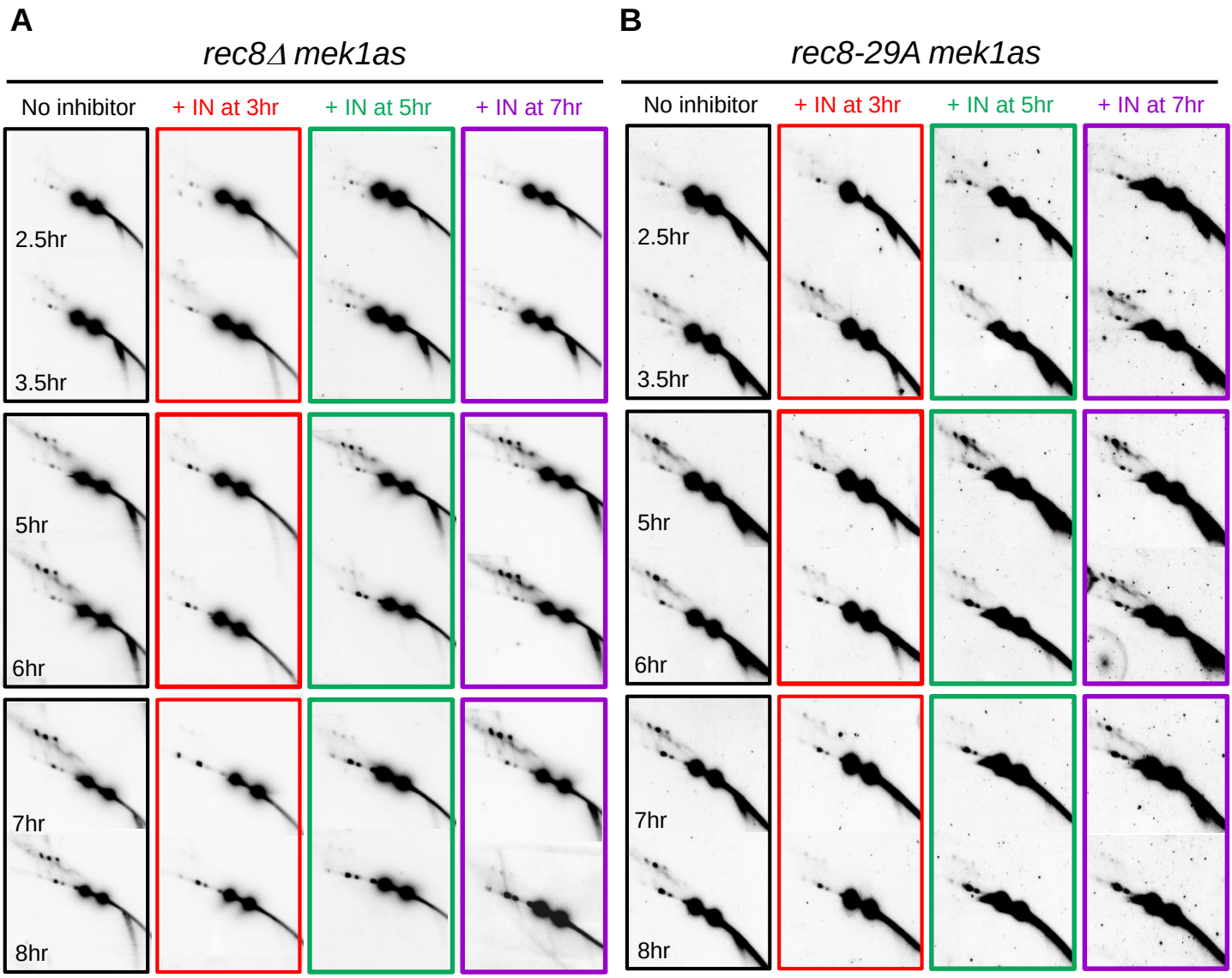
A
rec8Δ mek1as
No inhibitor
+ IN at 3hr
+ IN at 5hr
+ IN at 7hr
2.5hr
3.5hr
5hr
6hr
7hr
8hr
B
rec8-29A mek1as
No inhibitor
+ IN at 3hr
+ IN at 5hr
+ IN at 7hr
2.5hr
3.5hr
5hr
6hr
7hr
8hr

Figure S15

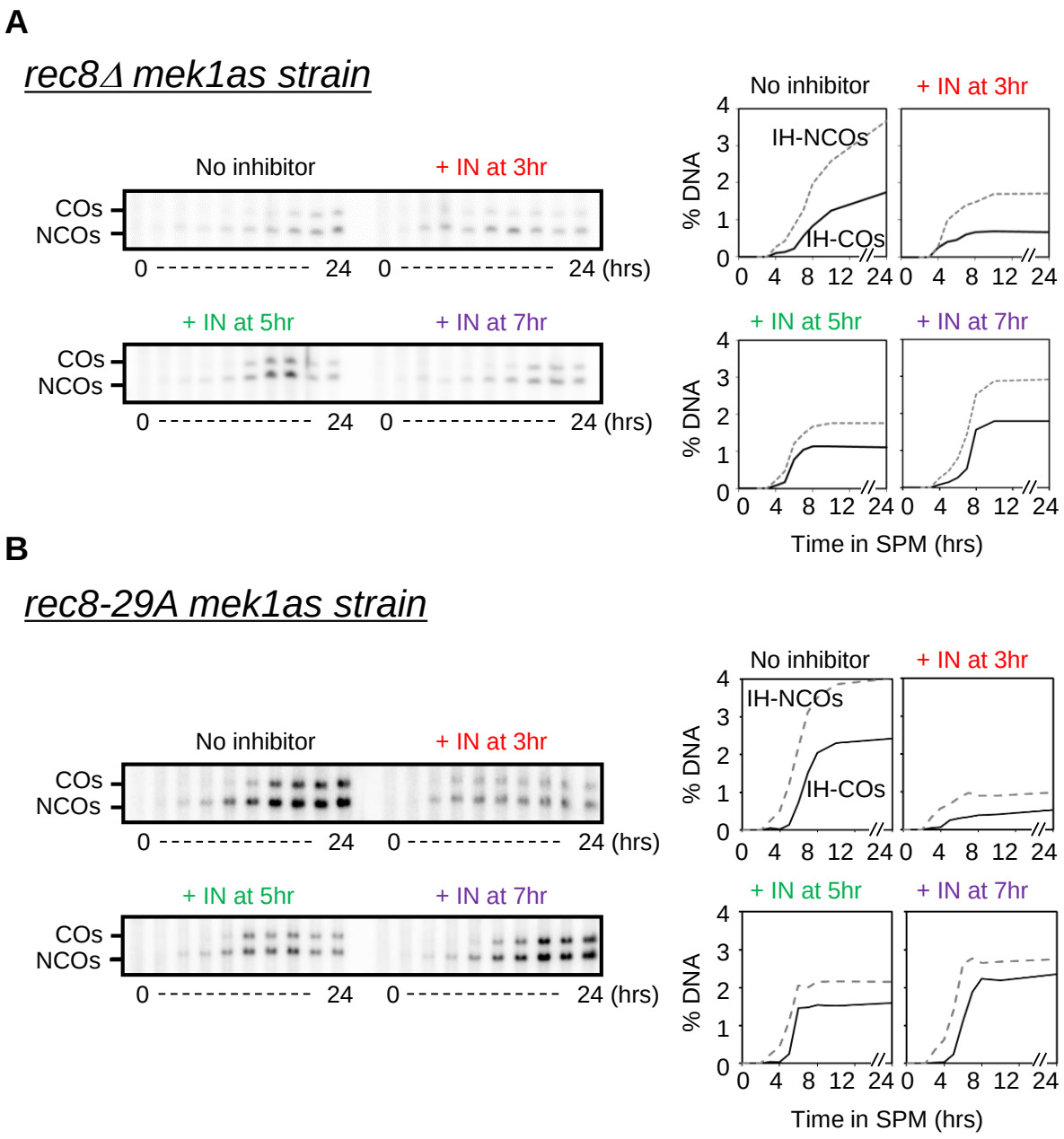
A
rec8Δ mek1as strain
No inhibitor
+ IN at 3hr
COs
NCOs
0
24
24 (hrs)
+ IN at 5hr
+ IN at 7hr
IH-NCOs
IH-COs
% DNA
Time in SPM (hrs)
B
rec8-29A mek1as strain

Figure S16

All strains are *rec8-6A mek1as*

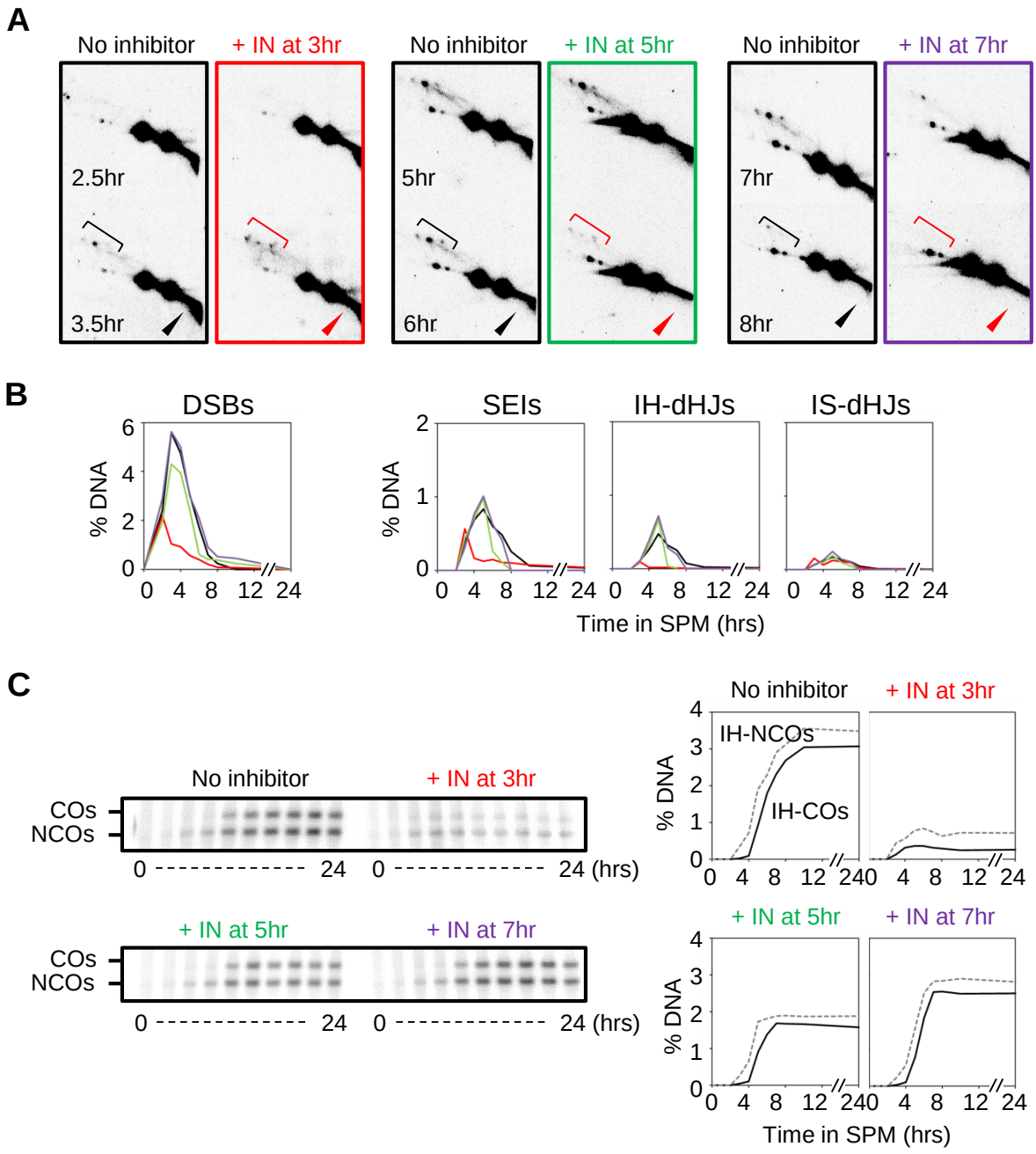

SUPPLEMENTARY FIGURE LEGENDS, REFERENCES, AND TABLE

Supplementary Figure S1. Rec8 phosphorylation and mutation sites. (**A**) Phosphorylation sites for serines, tyrosines, and threonines in *rec8-6A* (upper panel) and *rec8-29A* (bottom panel). (**B**) Immunoblot detection of Rec8 phosphorylation in protein extracts from WT, *rec8-6A*, and *rec8-29A* strains. Meiotic cells were harvested at 6 h in SPM cultures. Pgk1 was served as a loading control. PPase, protein phosphatase.

Supplementary Figure S2. Physical analysis of meiotic recombination in the Rec8 non-cleavable (*rec8N*) strain. (**A**) *URA3-arg4* recombination reporter system. Diagrams showing loci carrying the *URA3-ARG4* and *URA3-arg4EcPal9* reporter construct, as well as characteristic species detected by Southern blotting against *Xho*I or *Xho*I/*Eco*RI-digested meiotic DNA with *ArgD* or *hisU*-specific probes, respectively. (**B**) *Xho*I *ArgD* Southern blots with meiotic time-course samples from WT and *REC8N* strains containing the *URA3-arg4* reporter. (**C**) *his4::URA3-arg4* parent specific *Xho*I/*EcoR*I *hisU* Southern blots on the same DNA samples that were assayed in panel B. The DSB1 fragment ran at ~2.8kb due to the DSB1 proximal *EcoR*I site being rendered single stranded and thus recalcitrant to cleavage by *EcoR*I, with the next *EcoR*I site located 2.7kb upstream. The intact *HIS4* locus on the parent one chromosome was observed as a 0.6kb band. (**D**) Quantification of recombination intermediates and products of WT and *REC8N*. Blue: obtained from *Xho*I *ArgD* assays. Red: obtained from *Xho*I/*EcoR*I assays. *XhoI ArgD* intermediates were quantified against the sum of parent 1*,* parent 2, and derived species, and *Xho*I/*EcoR*I intermediates were quantified against *HIS4*. CO *Xho*I *ArgD* is the sum of CO1+CO2, CO *Xho*I/*EcoR*I *hisU* is CO1. (**E**) Meiotic progression in the time-course experiments assayed by Southern blotting. Exit from prophase I was assayed by following the spindle morphology via whole-cell immuno-staining through the meiotic time course. The solid line shows the fraction of cells with a monopolar

spindle, and the dashed line shows the fraction of bipolar spindles of meiosis I, indicating the transition from prophase I to metaphase I. One hundred cells were assayed per time point, except for t = 6h SPM with n = 200 - 300.

Supplementary Figure S3. DSB formation in the various loci. (**A**) 1D gel analysis of DSB formation at *BUD23*, *ARG4*, and *CYS3* loci. (**B**) Quantitative of DSB shown in (A).

Supplementary Figure S4. Meiotic recombination in the *rec8-24A* strain. (**A**) Serine and threonine phosphorylation sites in *rec8-24A*. (**B**) Southern blot of native/native two-dimensional (2D) gel images showing JMs. (**C**) Quantification of SEIs and dHJs in WT and *rec8-24A* cells (mean ± SEM, for three cultures). (**D**) One-dimensional (1D) gel analysis of interhomolog crossover (IH-CO) and interhomolog non-crossover (IH-NCO) formation. (**E**) Quantitative analysis of IH-CO and IH-NCO formation (mean ± SEM, for three cultures). (**F**) Comparison of maximal peak joint molecule (JM) and recombinant levels in WT and *rec8-24A* cells. Δ1/2 max is the time difference between the maximum values in WT and *rec8-24A*. (**G**). Meiotic division (% MI±MII) in WT and *rec8-24A* strains.

Supplementary Figure S5. Analysis of crossover at *ARG4*. (**A**) Genetic map of the *ARG4* locus and Southern blot probe (Goyon and Lichten, 1993). DNA species after digestion with *Bgl*II were indicated. (**B**) Southern blot images of crossover analysis in WT and Rec8 phospho-mutant strains. Time points are 0, 2.5, 3.5, 4, 5, 6, 7, and 8 hours. (**C**) Quantification of CO1 and CO2 at *ARG4* locus. Grey lines in *rec8-6A* and *rec8-29A* plots indicate COs of WT.

Supplementary Figure S6. Analysis of spore viability in WT and *rec8* phospho-mutant

strains. The population of tetrads for each strain with indicated viable spores (four, three, two, one and zero) was scored and exhibited as specified colors (WT, black; *rec8-6A*, purple; *rec8-29A*, brown). The vertical and horizontal axes represent the population of each dissected tetrad and the number of viable spores per one tetrad, respectively (n, the total number of dissected tetrads; S.V, the % of spore viability).

Supplementary Figure S7. Esp1 expression under the control of *CUP1* promoter in mitotic cells and meiotic cells. (**A**) Cells were synchronized in SPS for 18 hr at 30 °C incubator. The synchronized cells were then resuspended with YPD medium. Esp1 expression was induced by the addition of 50 μM $CuSO_4$ at 30 min after transferring the P_{CUP1}-*ESP1* strain to YPD. (**B**) Cells were synchronized in SPS medium as shown in (A). The cultures were transferred in SPM medium to initiate meiosis. Then, to express Esp1, 50 μM $CuSO_4$ was added to the culture at 2 hr after transferring the P_{CUP1}-*ESP1* strain to SPM.

Supplementary Figure S8. Rec8 cleavage by ectopic expression of Esp1 in *NDT80*, *ndt80Δ*, *rec8-29A,* and P_{CUP1}-*Esp1 rec8-24A* strains. (**A**) Ectopic expression of Esp1 induces Rec8 cleavage during meiosis. Extracts were prepared from meiotic P_{CUP1}-*ESP1* cells in the presence (right panel, t = 2 hr) or absence (left panel) of $CuSO_4$. (**B**) Ectopic expression of Esp1 induces Rec8 cleavage before pachytene exit. Protein extracts were prepared from *ndt80Δ* P_{CUP1}-*ESP1* cells in the presence (right panel, t = 2hr) or absence (left panel) of $CuSO_4$. (**C** and **D**) Rec8 cleavage in P_{CUP1}-*Esp1 rec8-29A* and P_{CUP1}-*Esp1 rec8-24A*. Protein extracts were prepared from meiotic P_{CUP1}-*ESP1 re8-29A* (**C**) and P_{CUP1}-*ESP1 rec8-29A* (**D**) cells in the presence (right panel, t = 2 hr) or absence (left panel) of $CuSO_4$ and Rec8-3HA proteins were detected using anti-HA antibody by western blotting.

Supplementary Figure S9. Analysis of meiotic recombination in P_{CUP1}-*Esp1* cells. (**A**) Normalized curves to compare the timing of CO, meiotic division, and sister separation from the analysis shown in Figure 2B and Figure 4. Dashed lines indicate crossover kinetics of WT. (**B**) 1D gel analysis of DSB formation. (**C**) 2D gel analysis of SEI and dHJ formation. (**D**) Analysis of IH-COs and IH-NCOs.

Supplementary Figure S10. DNA replication and meiotic division curves in in *hrr25-as* and *cdc7-as3* mutant strains (**A**) DNA replication in *hrr25-as* and *cdc7-as3* mutant strains in the presence or absence of chemical inhibitor. (**B**) Meiotic division in *hrr25-as* and *cdc7-as3* strains in the presence or absence of chemical inhibitor. (**C**) Southern analysis of COs and NCOs at *HIS4LEU2*.

Supplementary Figure S11. Rec8 cleavage at early prophase I exhibits defects in meiotic recombination. Representative southern blot images of 2D gel analysis and quantification of JM levels. (**A**) Representative 2D gel images for *ndt80Δ* P_{CUP1}-*CDC5* strain in the presence or absence of $CuSO_4$. 50 μM $CuSO_4$ was added directly to one of the two cultures at 7h, and the cultures were then analyzed in parallel through meiosis to compare directly -Cdc5 (-$CuSO_4$) and +Cdc5 (+$CuSO_4$) results. (**B**) Quantitative analysis of DSBs, SEIs, dHJs, IH-COs, and IH-NCOs. IH-CO and IH-NCO products were evaluated by *Xho*I and *NgoM*IV restriction polymorphisms (See Figure 1D). Vertical dash lines indicate the time of $CuSO_4$ addition.

Supplementary Figure S12. Formation of crossover and non-crossover in WT, *rec8-29A*, *zip1Δ*, *zip1Δ rec8-29A*, *zip3Δ*, *zip3Δ rec8-29A* mutants. (**A**) Southern blot images of crossover and non-crossover analysis in indicated strains. (**B**) Quantification of crossover

and non-crossover.

Supplementary Figure S13. Analysis of JMs in *mek1as* and *rec8Δ mek1as* mutants at 23 °C in the presence or absence of 1-NA-PP1. For 23 °C experiments, pre-meiotic cultures (SPS) were transferred to SPM medium to 30 °C; then after 2.5hr, meiotic cultures were shift to 23 °C incubator. (**A**) Representative 2D-gel images of JMs. (**B**) Quantitation analysis for DSBs and JMs. (**C**) Quantification analysis of IH-COs and -IHNCOs.

Supplementary Figure S14. Southern blot analysis of two-dimensional (2D) gels of samples taken during progression through meiosis. (**A** and **B**) The gel images show JM analysis of *rec8Δ mek1as* and *rec8-29A mek1as* strain in the presence or absence of Mek1 kinase inhibitor at the indicated times.

Supplementary Figure S15. Formation of IH-COs and IH-NCOs is dependent on Mek1 kinase inactivation. (**A**) Analysis of IH-CO and IH-NCO formation in the *rec8Δ mek1as* strain. Representative images of COs and NCOs (left panel) and the corresponding quantitation data (right panel). (**B**) Patterns of IH-CO and IH-NCO formation in the *rec8-29A mek1as* strain. Representative images of IH-COs and IH-NCOs (left panel) and corresponding quantitation data (right panel).

Supplementary Figure S16. Analysis of recombination patterns with the *rec8-6A mek1as* strain. (**A**) Representative images from a 2D-gel of *rec8-6A mek1as* in the presence or absence of 1-NA-PP1 at the indicated time points. Square brackets and arrowheads denote JMs and DSBs, respectively. (**B**) Quantification analysis of recombination intermediates in the *rec8-6A mek1as* strain shown in panel A. (**C**) Patterns of IH-CO and IH-NCO formation. Representative images of IH-COs and IH-NCOs (left panel) and corresponding quantitation

data (right panel).

Supplemental Reference

Goyon, C. and Lichten, M. (1993) Timing of molecular events in meiosis in Saccharomyces cerevisiae: stable heteroduplex DNA in formed late in meiotic prophase. *Mol*. *Cell*. *Biol*., **13**, 373-382.

153 Supplementary Table 1. Yeast strains used in this study.

Strain†	Genotype‡
KKY276	*MATa/MATα HIS4::LEU2-(BamHI)/his4x::LEU2-(NgoMIV)--URA3*
KKY109	*MATa/MATα HIS4::LEU2-(BamHI)/his4-x::LEU2-(NgoMIV)--URA3, rad50s::URA3/"*
KKY110	*MATa/MATα HIS4::LEU2-(BamHI)/his4-x::LEU2-(NgoMIV)--URA3, rad50s::URA3/", rec8Δ::KanMX4/"*
KKY1784	*MATa/MATα HIS4::LEU2-(BamHI)/his4-x::LEU2-(NgoMIV)--URA3, rec8Δ::KanMX4::rec8-6A-3HA::LEU2/", rad50s::URA3/"*
KKY1744	*MATa/MATα HIS4::LEU2-(BamHI)/his4-x::LEU2-(NgoMIV)--URA3, rec8Δ::KanMX4::rec8-29A-3HA::LEU2/", rad50s::URA3/"*
KKY179	*MATa/MATα HIS4::LEU2-(BamHI)/his4-x::LEU2-(NgoMIV)--URA3, rec8Δ::KanMX4::rec8-6A-3HA::LEU2/"*
KKY173	*MATa/MATα HIS4::LEU2-(BamHI)/his4-x::LEU2-(NgoMIV)--URA3, rec8Δ::KanMX4::rec8-29A-3HA::LEU2/"*
KKY1080	*MATa/MATα HIS4::LEU2(BamHI)/his4-x::LEU2-(NgoMIV)—URA3, rec8Δ::KanMX4/"*
KKY1933	*MATa/MATα HIS4::LEU2-(BamHI)/his4-x::LEU2-(NgoMIV)--URA3, ndt80Δ::KanMX4/", KanMX6-pCUP1-3HA-CDC5*
KKY2029	*MATa/MATα HIS4::LEU2-(BamHI)/his4-x::LEU2-(NgoMIV)—URA3, ZIP3-13myc::HygB/ZIP3*
KKY2030	*MATa/MATα HIS4::LEU2-(BamHI)/his4x::LEU2-(NgoMIV)—URA3, ZIP3-13myc::HygB/ZIP3, rec8Δ::KanMX4/"*
KKY2031	*MATa/MATα HIS4::LEU2-(BamHI)/his4x::LEU2-(NgoMIV)—URA3, ZIP3-13myc::HygB/ZIP3, rec8Δ::KanMX4::rec8-6A::LEU2/"*
KKY2032	*MATa/MATα HIS4::LEU2-(BamHI)/his4x::LEU2-(NgoMIV)—URA3, ZIP3-13myc::HygB/ZIP3, rec8Δ::KanMX4::rec8-29A::LEU2/"*
KKY1053	*MATa/MATα HIS4::LEU2-(BamHI)/his4-x::LEU2-(NgoMIV)--URA3, zip1Δ::KanMX4/"*
KKY1642	*MATa/MATα HIS4::LEU2-(BamHI)/his4x::LEU2-(NgoMIV)--URA3, zip1Δ::KanMX4/", rec8Δ::KanMX4::rec8-29A-3HA::LEU2/"*
KKY1054	*MATa/MATα HIS4::LEU2-(BamHI)/his4-x::LEU2-(NgoMIV)--URA3, zip3Δ::KanMX4/"*
KKY1650	*MATa/MATα HIS4::LEU2-(BamHI)/his4-x::LEU2-(NgoMIV)--URA3, zip3Δ::KanMX4/", rec8Δ::KanMX4::rec8-29A-3HA::LEU2/"*
KKY2278	*MATa/MATα KanMX4-pCUP1-ESP1/", REC8-3HA::URA3/"*
KKY2296	*MATa/MATα URA3::CYC1p-LacI-GFP, scp1(Ch XV telomere)::LacO-LEU2, KanMX4-pCUP1-ESP1/"*
KKY2256	*MATa/MATα HIS4::LEU2-(BamHI)/his4-x::LEU2-(NgoMIV)--URA3, KanMX4-pCUP1-ESP1/"*
KKY2342	*MATa/MATα HIS4::LEU2-(BamHI)/his4-x::LEU2-(NgoMIVi)--URA3, REC8N-3HA::KanMX::LEU2/"*
KKY202	*MATa/MATα HIS4::LEU2-(BamHI)/his4x::LEU2-(NgoMIV)-URA3,*

	rec8-24SA-HA3::LEU2::rec8Δ::KanMX4/"
KKY194	*MATa/MATα HIS4::LEU2-(BamHI)/his4-x::LEU2-(NgoMIV)--URA3, rec8Δ::KanMX4/", mek1::LEU2::mek1-as1::URA3/"*
KKY857	*MATa/MATα HIS4::LEU2-(BamHI)/his4-x::LEU2-(NgoMIV)--URA3, rec8Δ::KanMX4::rec8-29A-3HA::LEU2/", mek1::LEU2::mek1-as1::URA3/"*
KKY197	*MATa/MATα HIS4::LEU2-(BamHI)/his4-x::LEU2-(NgoMIV)--URA3, mek1::LEU2::mek1-as1::URA3/",*
KKY856	*MATa/MATα HIS4::LEU2-(BamHI)/his4-x::LEU2-(NgoMIV)--URA3, rec8Δ::KanMX4::rec8-6A-3HA::LEU2/", mek1::LEU2::mek1-as1::URA3/"*
KKY2324	*MATa/MATα HIS4::LEU2-(BamHI)/his4-x::LEU2-(NgoMIV)—URA3, pCUP1-KanMX-Esp1/", REC8-3HA::URA3/", ndt80Δ::KanMX4/"*
FKY3061	*MATa/MATα ho::LYS2/", lys2/", arg4Δ(eco47III-hpa1)/", leu2-R/leu2-RV::URA3-(Sma1-Eco47III)-ARG4, his4Δ (Sal1-Cla1)::URA3-Δ (Sma1-Eco47III)-arg4-EcPal(1691)/HIS4, REC8N-HA3::LEU2/"*
FKY3108	*MATa/MATα ho::LYS2/", lys2/", arg4Δ (eco47III-hpa1)/", leu2-R/leu2-RV::URA3-(Sma1-Eco47III)-ARG4, his4Δ (Sal1-Cla1)::URA3-Δ (sma1-eco47III)-arg4-EcPal(1691)/HIS4*
KKY2278	*MATa/MATα pCUP1-KanMX-Esp1/", REC8-3HA::URA3/"*
KKY2324	*MATa/MATα pCUP1-KanMX-Esp1/", REC8-3HA::URA3/", ndt80Δ::KanMX4/"*
KKY1603	*MATa/MATα HIS4::LEU2-(BamHI) / his4-x::LEU2-(NgoMIV)--URA3, pCUP1-KanMX-ESP1/", rec8Δ::KanMX4::Rec8-29A::LEU2/"*
KKY1597	*MATa/MATα HIS4::LEU-(BamHI) / his4-x::LEU2-(NgoMIV)--URA3, pCUP1-KanMX-ESP1/", Rec8-24SA-HA3::LEU2/", rec8Δ::KanMX4/",*
KKY2420	*MATa/MATα pCUP1-KanMX-ESP1-9myc-Hyg/", MCD1-6HA-KanMX/"*
KKY2378	*MATa/MATα HIS4::LEU2-(BamHI) / his4-x::LEU2-(NgoMIV)--URA3, cdc7-as3-myc/"*
KKY2500	*MATa/MATα HIS4::LEU2-(BamHI) / his4-x::LEU2-(NgoMIV)--URA3, Hrr25-as1-HIS3::hrr25Δ::KanMX4/"*
KKY2649	*MATa/MATα HIS4::LEU2-(BamHI) / his4-x::LEU2-(NgoMIV)-URA3, cdc7-as3-myc/", Hrr25-as1-HIS3::hrr25Δ::KanMX4/"*
KKY2471	*MATa/MATα arg4-bglII (nsp-) / arg4-nsp (nsp-), DED82-URA3-DED81*
KKY2490	*MATa/MATα arg4-bglII (nsp-) / arg4-nsp (nsp-), DED82-URA3-DED81, rec8Δ::KanMX4::Rec8-6A::LEU2/"*
KKY2491	*MATa/MATα arg4-bglII (nsp-) / arg4-nsp (nsp-), DED82-URA3-DED81, rec8Δ::KanMX4::Rec8-29A::LEU2/"*

† All strains are isogenic derivatives of SK1 background.

‡ All strains are also homozygous for the mutation *ho::hisG and leu2::hisG* (except FKY strains), and for *ura3 (ΔPstI-SmaI).*

157

158 Supplementary Table 2. Summary of mutant phenotypes in meiotic recombination

Genotypes	Relative *rad50S* DSB level	DSB hyperresection	IH:IS dHJ ratio[a]	CO level[b]	NCO level[b]	CO:NCO ratio	DSB timing	post-DSB progression
WT	= 1	= wt; normal	5.35:1	4.1	3.7	1.11:1	= wt	= wt
pCUP1-ESP1 [no $CuSO_4$]	not tested	= wt	4.8:1	3.9	3.5	1.12:1	= wt	= wt
rec8Δ	~0.8	modest	1.04:1	1.26	3.15	0.42:1	delay	delay
pCUP1-ESP1 +$CuSO_4$ [2hr]	not tested	modest	1.3:1	1.66	2.4	0.68:1	delay	delay
rec8-6A	~1	= wt	4.4:1	3.4	3.7	0.93:1	= wt	delay
rec8-24A	~1	= wt	4.1:1	2.8	3.7	0.75:1	= wt	delay
rec8-29A	~1	= wt	2.5:1	2.4	4.2	0.57:1	= wt	delay
cdc7-as3 [5hr]	not tested	= wt	not tested	1	1.3	0.78:1	none	none
hrr25-as cdc7-as3 [5hr]	not tested	= wt	not tested	0.76	1	0.67:1	none	none

159 [a] Average IH:IS ratio is shown for time points when dHJs were at maximal levels.

160 [b] Data are shown only for time points when CO and NCO were at maximal levels.

161